

# Near-shore submarine permafrost of the central Laptev Sea, East Siberia

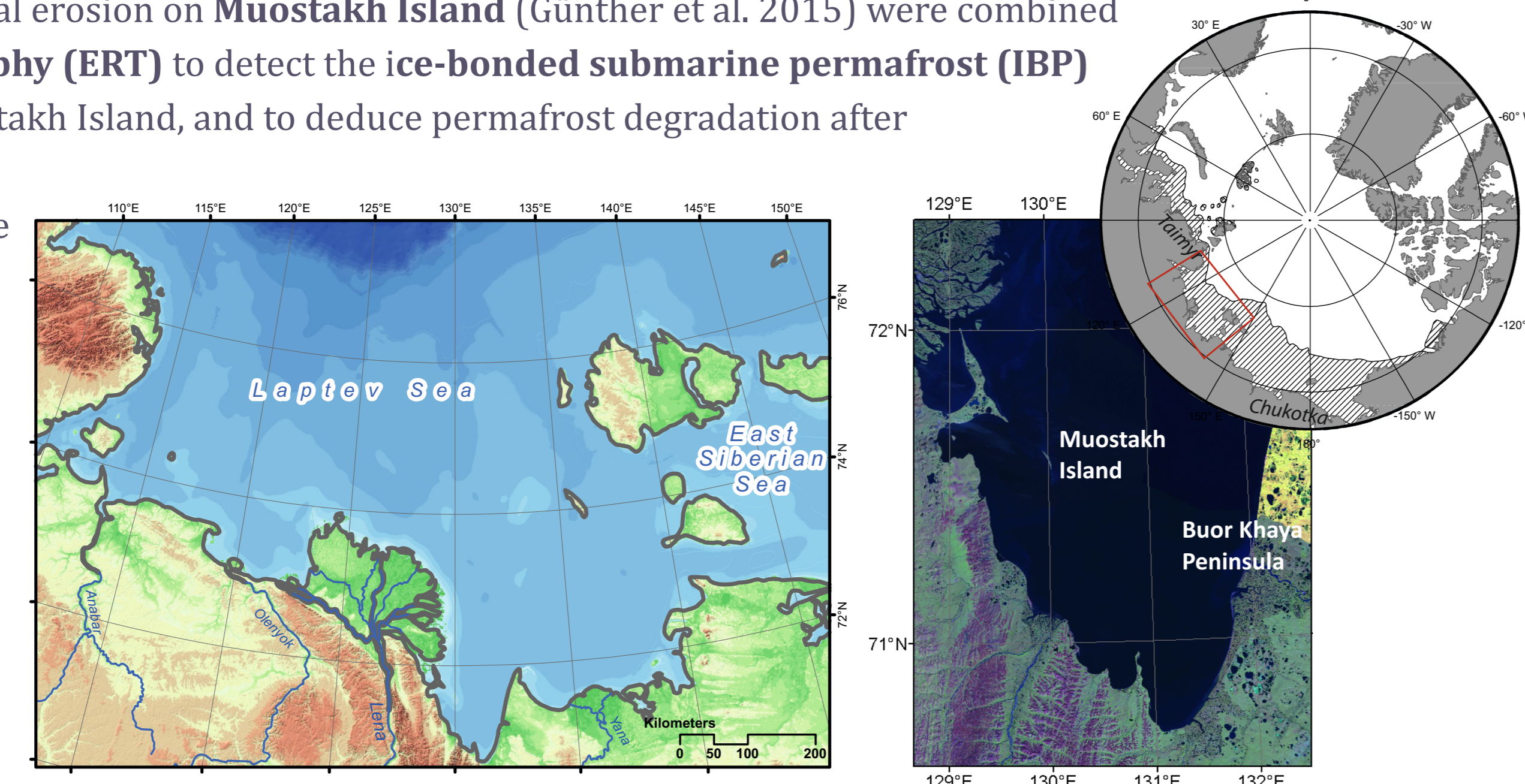
C43A-0769

Sebastian Wetterich<sup>1</sup>, Paul Overduin<sup>1</sup>, Frank Günther<sup>1</sup>, Susanne Liebner<sup>2</sup>, Christian Knoblauch<sup>3</sup>, Mikhail N. Grigoriev<sup>4</sup>, Lutz Schirrmeister<sup>1</sup>, Hans-Wolfgang Hubberten<sup>1</sup>

## 1 The Laptev Sea

Two study sites in the the **central Laptev Sea** (Fig. 1) were studied for (1) the relation between coastal retreat and submarine permafrost dynamics, and (2) for biogeochemical characteristics of submarine permafrost. Long-term on-site estimates of coastal erosion on **Muostakh Island** (Günther et al. 2015) were combined with **electrical resistivity tomography (ERT)** to detect the **ice-bonded submarine permafrost (IBP)** table in the near-shore zone of Muostakh Island, and to deduce permafrost degradation after inundation (Overduin et al. 2015a). Subsea permafrost drilling took place off-shore **Buor Khaya Peninsula** to obtain core material for further biogeochemical analyses to uncover **carbon stock and turnover** in thawing submarine permafrost (Overduin et al. 2015b).

Figure 1. Study area on the East Siberian Shelf.



## 2 Coastal erosion and submarine permafrost

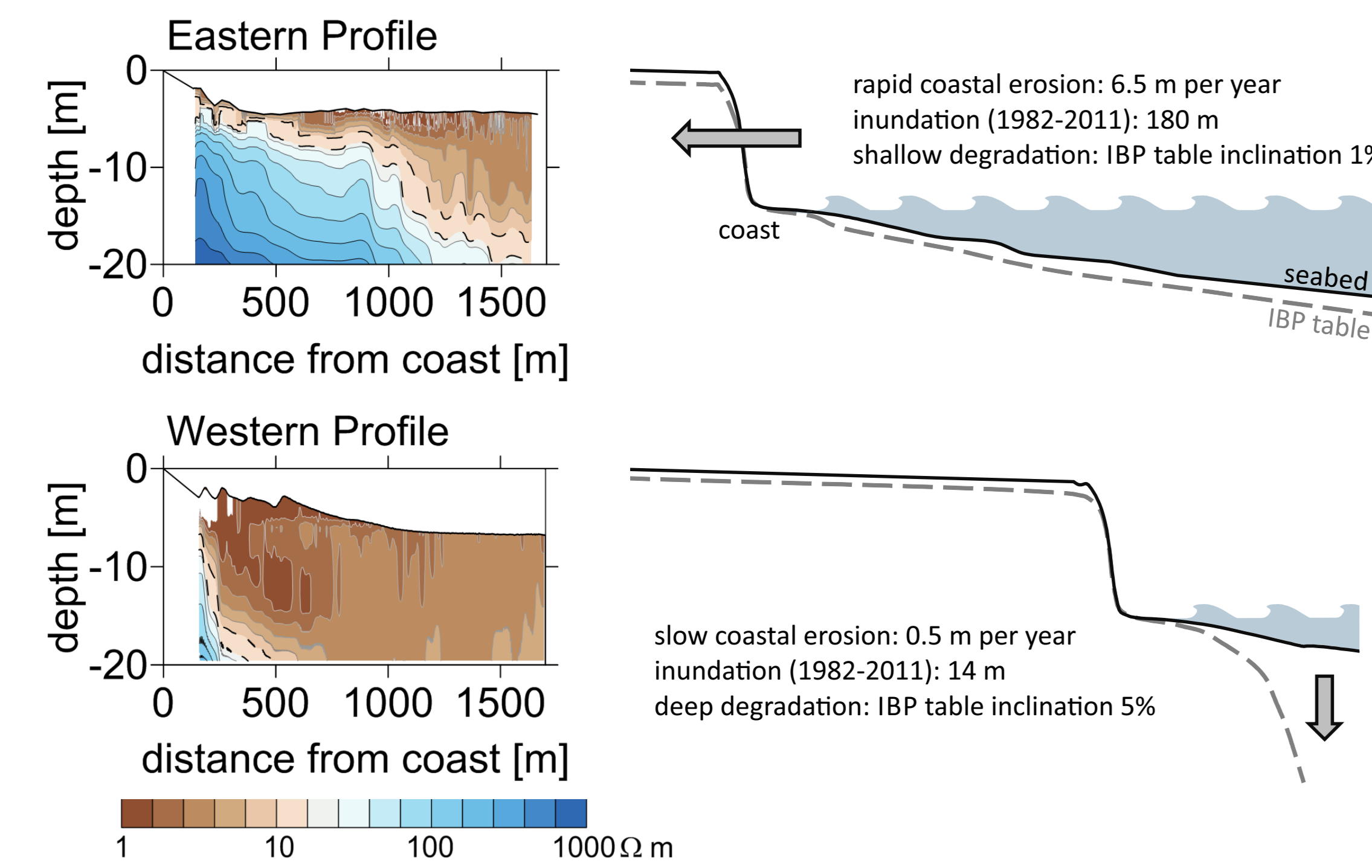


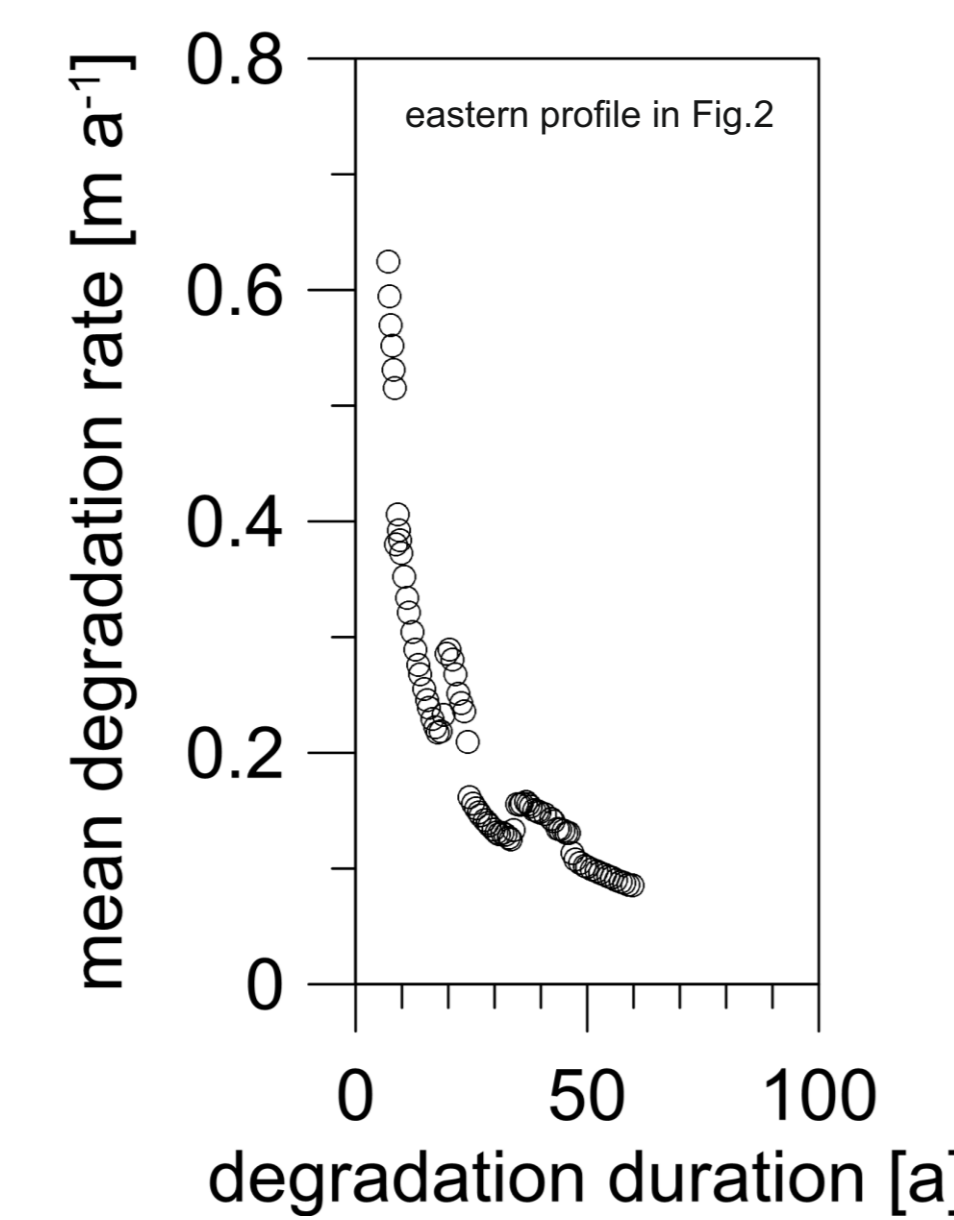
Figure 2. Inversions of the georesistivity profiles of the eastern and western Muostakh Island at positions with high and low coastal erosion rates, respectively. The relative rates of coastline retreat and permafrost degradation affect the shape of the IBP table beneath the shoreface profile.

**ERT surveys** (IRIS Syscal Pro™ Deep Marine system; RES2DINV™ software) were combined with bathymetry measurements to invert for sub-bottom georesistivity indicating **depths of saline sediment and underlying IBP**. The change in georesistivity from unfrozen seawater-saturated sediment to frozen ice-saturated sediment corresponds to a jump from less than 10 to over 100 Ωm (uncertainty in IBP depth taken at 10 to 20 Ωm, Fig. 2).

Submarine IBP degrades most rapidly immediately after it is inundated year-round. **Degradation rates slow over time** as the thermal and solute concentration gradients between the sea floor and the IBP table become less steep, decreasing fluxes of heat and salt, respectively.

The duration of inundation of points distal to the island are approximately 260 years on the eastern profile, and closer to 3500 years on the western profile (Fig. 2; based on profile length of 1700 m and coastal retreat rates of 0.5 and 6.5 m per year, respectively). It is likely that **degradation rates** for most of the East Siberian Shelf are **less than 0.1 m per year**.

Figure 3. Permafrost degradation rate inferred from geoelectric sounding depth and position for the eastern geoelectric profile (see Fig. 2). Data are shown for soundings at locations flooded since 1951.



## 3 Submarine permafrost drilling

**Sediment drilling** was conducted just offshore of the eastern coast of **Buor Khaya Bay** (Fig. 4), in April–May 2012. Casing was drilled through the sea ice into the seabed, allowing dry drilling using a **rotary drill with 4 m casing**. Drilling from a 2 m thick sea ice cover, 35 m of core were recovered between 2 and 48 m below sea floor (bsf) with a recovery rate of 78.4%. The borehole was located approximately 750 m from the modern coastline in 4 m deep water. **Ice-bonded sediment** was encountered at **24.75 m bsf**, with 24.7 m of overlying unfrozen sediment. The sharp boundary between unfrozen and frozen sediments was recovered within one core section. Borehole temperature was measured for 4 days.

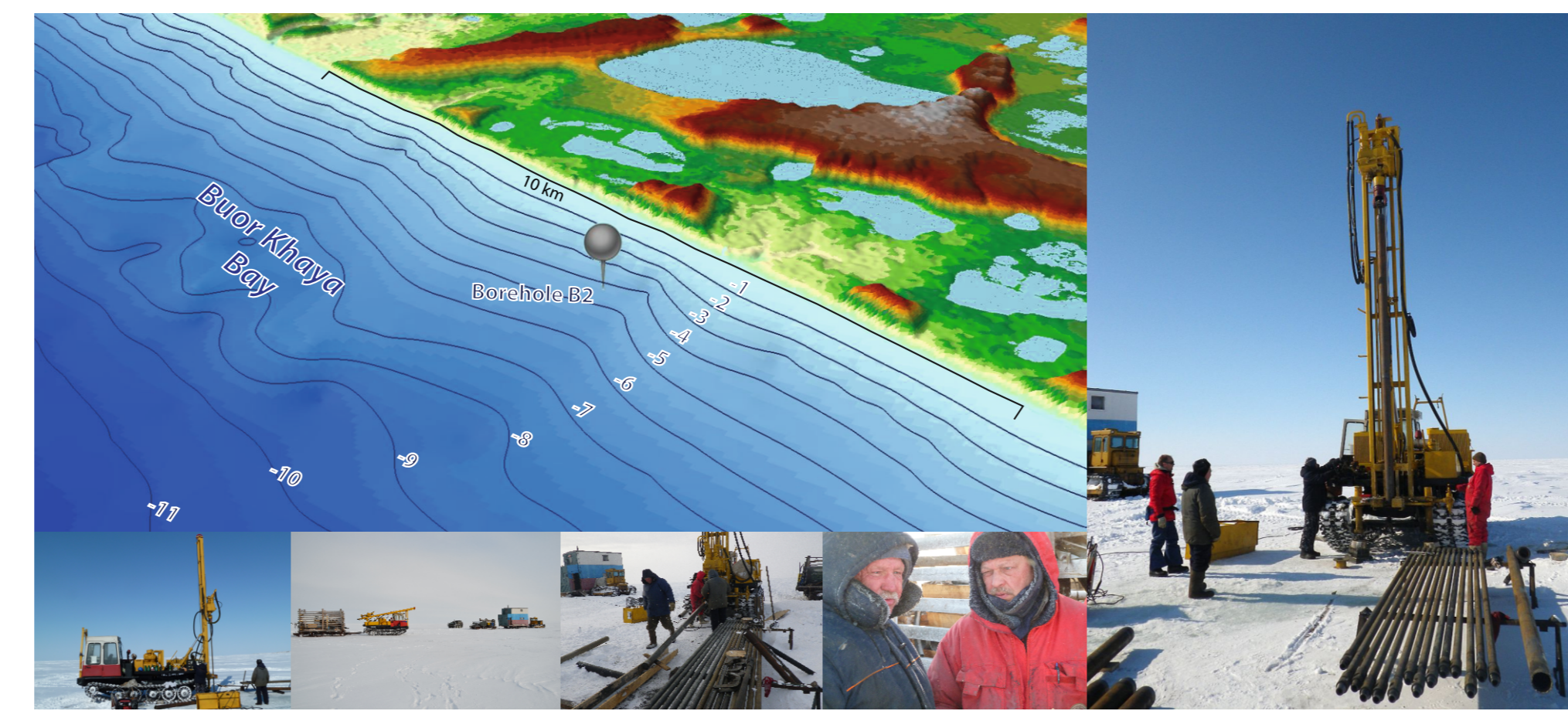


Figure 4. Drill site of the submarine permafrost core BK-2 at 71°25'20.3"N, 132°05'05.3"E. Some impressions of the fieldwork, the colleagues and the Russian drill auger URB-4T which allowed for core diameters between 7 and 12 cm.

## 4 Core data

Based on **cryostratigraphy** of the core, laboratory work focused on **carbon-related properties** of the IBP and the overlying unfrozen deposits. Main down-core results are summarised in Fig. 5.

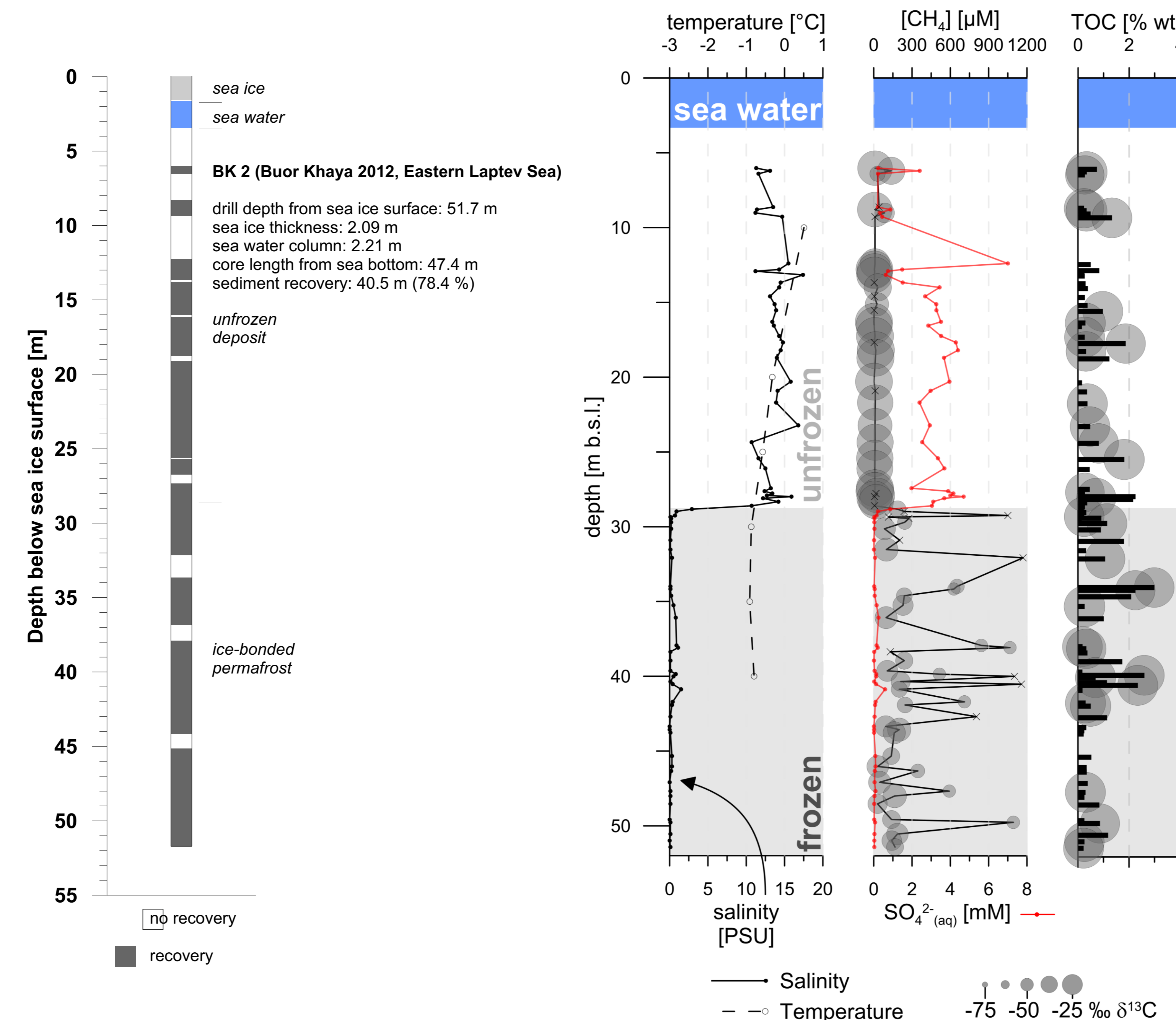
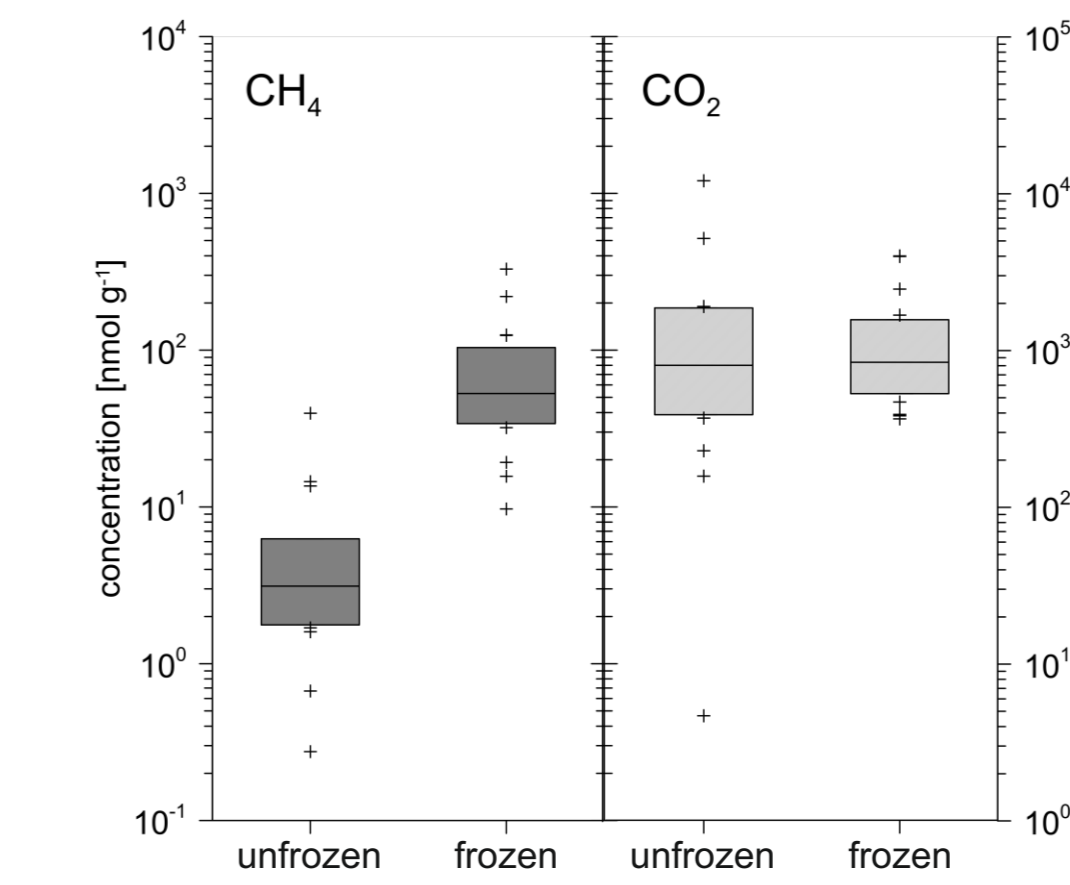


Figure 5. Borehole temperature and pore water characteristics (salinity and sulphate) as a function of core depth in comparison to methane concentration (CH<sub>4</sub>), total organic carbon (TOC) content and δ<sup>13</sup>C ratios of methane (δ<sup>13</sup>C-CH<sub>4</sub>) and of sediment total organic carbon (δ<sup>13</sup>C-TOC).

## 5 Methane turnover



The **IBP table is clearly defined** by changes in the presence/absence of ice, pore water salinity and related changes in pore water chemical and isotopic composition, and methane concentrations and δ<sup>13</sup>C-CH<sub>4</sub> signatures (Fig. 5).

While methane concentrations differ between frozen and unfrozen deposits, carbon dioxide concentrations are similar in both (Fig. 6).

Figure 6. The distribution of measured methane and carbon dioxide concentrations in frozen (IBP) and unfrozen deposits.

Coastal retreat of  $1.4 \pm 0.8$  m per year at the Buor Khaya coast indicates inundation of the drill site around 540 years ago. The **IBP degradation rate** amounts to  $5.3 \pm 2.7$  cm per year to reach the current IBP table at 24.75 m bsf.

**Methane release rates of  $121 \pm 64$  mg m<sup>-2</sup> per year** were calculated from thawing submarine permafrost.

Low methane concentration and high sulphate concentration above the IBP table indicate **sulphate-driven anaerobic oxidation of methane**, producing CO<sub>2</sub> and sulphide (S<sup>2-</sup>) upon permafrost thaw (Fig. 7).

Consequently, upward **methane migration** into the overlying sediment seems unlikely and methane release from the seabed does not derive from the degrading submarine permafrost (see e.g. Shakhova et al. 2010) but is **probably associated with methane from other sources** that can permeate through permafrost-free sediment.

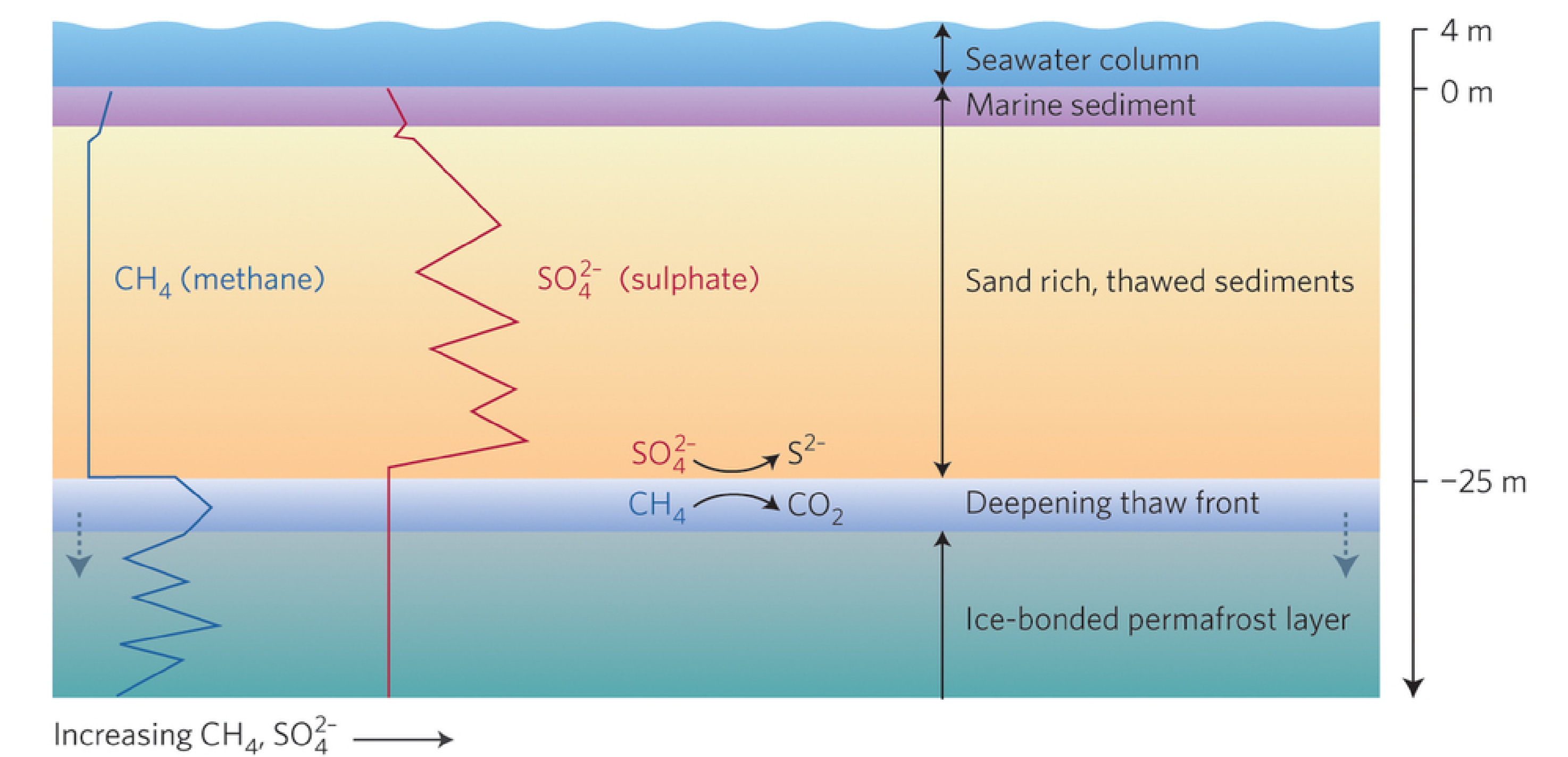


Figure 4. Summary scheme by Thornton and Crill (2015) to highlight the main downcore pattern of low methane and high sulphate of unfrozen deposits compared to higher methane and lower sulphate of ice-bonded permafrost, indicating efficient sulphate-driven anaerobic oxidation of methane at the deepening thaw front.

## 6 Conclusions

**Subsea permafrost degradation triggered by duration since inundation which is a function of coastal retreat.**

**Long-term degradation rates decrease over time as the depth to the IBP increases and thermal and pore water solute concentration gradients over depth decrease.**

**Methane concentrations in the IBP higher than those in the overlying unfrozen sediment.**

**Methane release upon thaw at a rate of  $121 \pm 64$  mg m<sup>2</sup> yr<sup>-1</sup> and oxidation at or immediately following thaw.**

**Anaerobic oxidation of methane at the thaw front prevents further migration.**

References  
Günther et al. 2015. Observing Muostakh disappear: Permafrost thaw subsidence and erosion of a ground-ice-rich island in response to arctic summer warming and sea ice reduction. *The Cryosphere* 9, 151-178.  
Overduin et al., 2015a. Coastal dynamics and submarine permafrost in shallow water of the central Laptev Sea, East Siberia. *The Cryosphere Discussions* 9, 3741-3775.  
Overduin et al., 2015b. Methane oxidation following submarine permafrost degradation: Measurements from a central Laptev Sea shelf borehole. *Journal of Geophysical Research - Biogeosciences* 120, 965-978.  
Shakhova et al., 2010. Extensive methane venting to the atmosphere from the sediments of the East Siberian Arctic shelf. *Science* 327, 5970.  
Thornton BF, Crill P, 2015. Microbial lid on subsea methane. *Nature Climate Change* 5, 723-724.